International Journal of RF and Microwave Computer-Aided Engineering / Early View / e22880

RESEARCH ARTICLE | Free Access

Compact bio-inspired dual-band uniplanar electromagnetic bandgap-backed antenna for wearable applications

Jeremiah O. Abolade ✉, Dominic B. O. Konditi, Vasant. M. Dharmadhikary

First published: 26 August 2021
https://doi.org/10.1002/mmce.22880

Funding information: Pan African University Institute of Basic Sciences, Technology, and Innovation; African Union

Abstract

A compact bio-inspired electromagnetic bandgap integrated wearable antenna (Bio-EBG-iwA) is proposed in this work. The Bio-EBG-iwA is based on the hybridization of semi-*Vitis vinifera* leaf-shaped patch, asymmetric feedline, reflected G-shaped slot, partial ground, and a stub on the ground plane. The antenna is built on the locally made textile material called *Aso-oke* (Alari) with permittivity and a loss tangent of 1.43 and 0.019, respectively. The dimension of the proposed antenna is $0.2\ \lambda_g \times 0.1\ \lambda_g \times 0.0089\ \lambda_g$ (22 mm × 12 mm × 0.7 mm) at 2.45 GHz. Despite its compactness, the gain of −0.48 and 2.5 dBi are achieved at 2.45 and 5.7 GHz respectively without electromagnetic bandgap (EBG). A dual-band textile-based uniplanar compact electromagnetic bandgap (UC-EBG) is introduced to create isolation between the human tissue and the antenna. The dual-band UC-EBG is realized through the use of a modified slitted-square ring (MSSR) and the 90° rotated H-shaped patch on *Aso-oke* (Alari) with a thickness of 2.1 mm. The periodicity of the proposed UC-EBG is 34.5 mm. The antenna is placed on a 2 × 2 array of the proposed UC-EBG separated by a 3 mm foam thickness. The radiation efficiency of 88.97% and 79.85% are achieved at 2.45 and 5.7 GHz respectively. The gain of the proposed UC-EBG integrated antenna increased from −0.48 and 2.5 dBi to 5.9 and 10.7 dBi at 2.45 and 5.7 GHz, respectively. The front-to-back ratio (FBR) of 26.3 dB is achieved with the use of UC-EBG. The use of UC-EBG results in a 98.31% and 99.4% reduction in average SAR at 2.45 and 5.7 GHz, respectively. The off-body and on-body performance analysis of the proposed UC-EBG integrated antenna show that the proposed EBG integrated antenna (Bio-EBG-iwA) is a suitable candidate for wearable application. To

the best of our knowledge, this is the most compact wearable antenna with suitable gain, radiation efficiency, and high FBR. In addition, our proposed UC-EBG shows that slitting is an effective way of miniaturizing the EBG structure.

1 INTRODUCTION

The wearable antenna is becoming increasingly demanding in the wireless communication market in recent times due to the increase in the usage of wearable devices, in medicine, the Military, safety, sport, and so on.[1-5] With the outbreak of Covid-19, wearable devices are much needed in medical applications than ever before. Wearable antennas are much needed in medical, sport, and security applications for either on-body or in-body wireless communication. This group of communication is termed wireless body area networks (WBAN). Unlike the standard antennas, wearable antenna designers are faced with several issues, such as conformability, compactness, and back radiation issues, which greatly impaired the performance of the antenna as well as having a negative impact on the users when placed at proximity to the body.[6, 7] A wearable antenna should be compact enough for esthesis and conformability without affecting the antenna radiation efficiency. Several works have been done in this regard, yet, according to the literature reviewed, our proposed bio-inspired antenna is comparatively smaller than the recently published antenna without compromising the radiation efficiency. For example, authors in Ref. 6 proposed a monoband semi-flexible antenna on an RT/duroid 5880 with a dimension of 17 mm × 25 mm × 0.787 mm. In the same light, the authors in Ref. 8 proposed a monoband flexible wearable antenna on a Denim substrate with a dimension of 30 mm × 20 mm × 0.7 mm. Furthermore, a multiband antenna is proposed in Ref. 9 using a slanted monopole on polyester material with a dimension of 85 mm × 45.5 mm × 1 mm. Recently, authors in Ref. 10 proposed a wearable antenna using E-slot technique on a Jean substrate with a dimension of 20 mm × 30 mm × 0.7 mm. Comparatively, the dimension of the proposed Bio-EBG-iwA is 22 mm × 12 mm × 0.7 mm.

The introduction of EBG in antenna application by authors in Ref. 11 has led to the evolution of several innovative EBG designs. In terms of the number of bands, EBG can be categorized into a single, dual, and multi-band. EBG can also be categorized as 1-D, 2-D, and 3-D EBG which is based on the cells' arrangement. Finally, an EBG can be grouped in terms of design configuration such as Mushroom and uniplanar configuration.[10, 12] The commonly designed EBG is a single band with a 2-D configuration.[8, 10, 13-16] Dual-band EBGs have been proposed in the literature such as Refs. 17-19. For example, the authors in Ref. 17 proposed a dual-band mushroom-like EBG on an FR4 substrate. The design was based on a circular ring slot on the standard rectangular patch with a via at the center connecting the patch to the ground. The size of the unit cell is $0.27\ \lambda_g \times 0.27\ \lambda_g \times 0.04\ \lambda_g$ at 2.4 GHz. In addition, authors in Ref. 18 used circular ring slot on the circular patch in conjunction with two vias with different diameters

(small diameter via at the center and big diameter via at the edge). The choice of design configuration depends majorly on the application. For example, Uniplanar configuration is more desirable in wearable antenna due to the absence of vias and ease of fabrication. Therefore, a novel uniplanar EBG configuration is herein presented.

In this work, a semi-*Vitis-vinifera* leaf-shaped slitted patch, with an asymmetric microstrip-fed dual-band wearable antenna is proposed. The compactness is achieved through the combination of asymmetric feeding, partial ground, and slitting techniques on the *Aso-oke* textile material called" Alari" which electric properties were first reported in Ref. 20. In order to reduce the back radiation and specific absorption rate, which consequently improves the gain, a novel EBG is proposed.

The rest of this manuscript is organized as follows: the antenna and EBG design and analysis are presented in Section 2; the antenna performance over EBG for both OFF-body and ON-body are presented in Section 3; Comparative analysis of the Bio-EBG-iwA is presented in Section 4 and the conclusion is given in Section 5.

2 BIO-INSPIRED ANTENNA AND UC-EBG DESIGN AND ANALYSIS

2.1 Bio-inspired antenna

The Bio-EBG-iwA is built on a wearable textile material called *Aso-oke* (Alari) with a dielectric permittivity and loss tangent of 1.43 and 0.019 respectively. The total dimension of the Bio-EBG-iwA is $22 \times 12 mm^2$ and a thickness of 0.7 mm. A typical *V. vinifera* leaf shape is as shown in Figure 1. The proposed structure begins with a semi *V. vinifera* leaf-shape monopole antenna as shown in Figure 2(A). A reflected modified G-shape slit is then embedded on the patch as shown in Figure 2(B). Finally, a stub is introduced on the monopole ground plane to enhance the impedance matching as shown in Figure 2(C). The optimized dimension of the proposed structure is as given in Table 1 and the point coordinates of the radiating semi *V. vinifera* leaf-shape is adopted from our former work and can be found in Ref. 21. The perimeter of the proposed antenna patch can be calculated from its coordinates using Equation (1).[21] The resonance of the Bio-EBG-iwA before the introduction of the reflected G-shape slit can be predicted using Equation (2).[21] The purpose of the slit is to create a band-notch and thereby produce a dual-band configuration. The band notch introduced by the proposed reflected G-shape slit can be predicted using Equations (4)–(7-4)–(7). Hence, a band-notch is expected at 2.6 GHz. Therefore, resonance is expected at the region below and above the notched frequency.

$$\psi = \sum_{n=1}^{N-1} \left[\sqrt{(x_{n+1} - x_n)^2 + (y_{n+1} - y_n)^2} \right]$$

(1)

$$f_r \approx \frac{300}{P\sqrt{\varepsilon_{\text{reff}}}}$$

(2)

where N = 46 from Table 2 of Ref. 21 and

$$\varepsilon_{\text{reff}} \approx \frac{\varepsilon_r + 1}{2}$$

(3)

The perimeter of the patch is denote by *P*, $\varepsilon_{\text{reff}}$ stands for the effective dielectric permittivity of the substrate,

$$f_{sl} = \frac{c_o}{4l_{sl}\sqrt{\varepsilon_{\text{reff}}}}$$

(4)

Where,

$$l_{sl} = 2\pi r_{sl} - g + L1 + L2$$

(5)

$$g = \frac{(\theta - \varphi)\text{x}2\pi r_{sl}}{\theta}$$

(6)

$$r_{sl} = R_{sl} + w$$

(7)

where, r_{sl} and R_{sl} are the outer and inner radius of the slit-arc respectively, w is the strip-width (0.5 mm), g is the arc-slit gap, θ is the angle of a circle (i.e., 360°), φ is the subtended angle of the arc-slit, $L1$ and $L2$ are the vertically and horizontally oriented rectangular part of the reflected G-shape slit as shown in Figure 3(C).

FIGURE 1

Open in figure viewer | PowerPoint

A typical Vine-leaf[21]

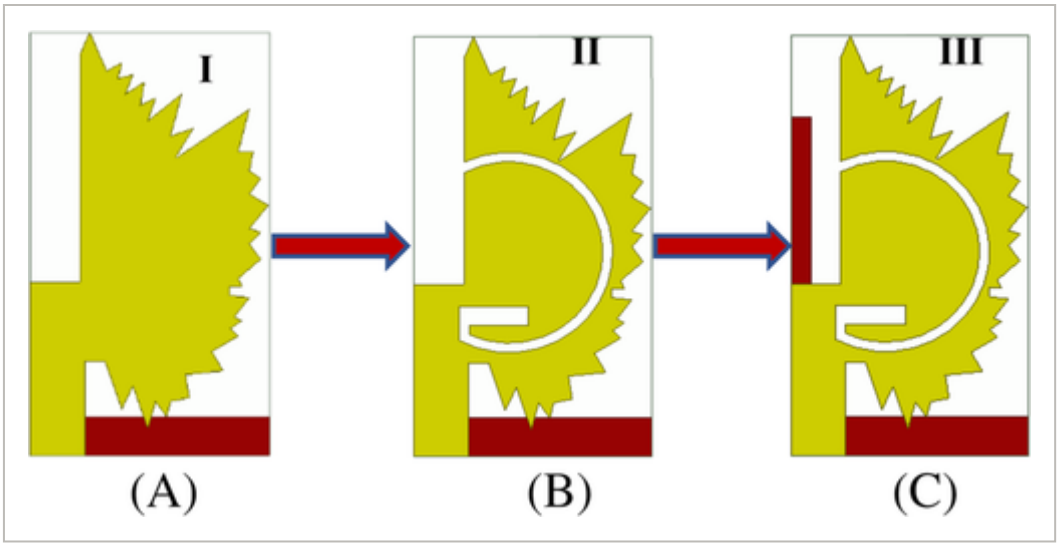

FIGURE 2

Open in figure viewer | PowerPoint

The iteration procedure of the proposed bio-inspired wearable antenna

TABLE 1. The optimized parameters of the bio-EBG-iwA structure

Parameter	W_{sub}	W_{st}	W_f	w	w_1	w_2	w_3	L_{sub}	L_{st}
Value (mm)	12	1	2.75	0.5	1	1	0.5	22	15.75
Parameter	L_g	L_f	L_1	L_2	L_3	L_4	R_{sl}	φ	
Value (mm)	2	9	1.9	3	5.87	5.46	5	236.57	

TABLE 2. The optimized parameter of the proposed UC-EBG

Parameter	W	w_1	w_2	w_3	w_4	w_5	w_6	w_7	L	l_1	l_2	l_3
Value (mm)	31.7	14.7	0.7	0.5	6.7	1.4	3.0	8.0	34.5	0.8	0.5	1.0

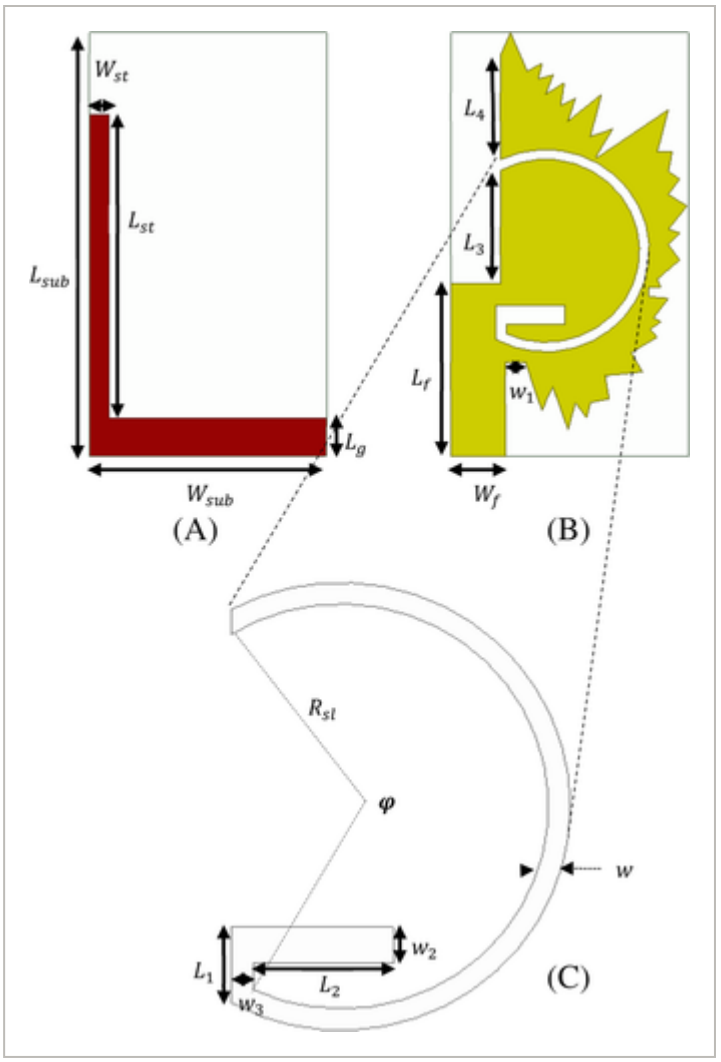

FIGURE 3

Open in figure viewer | PowerPoint

The proposed asymmetric microstrip-fed bio-inspired wearable antenna (A) bottom-view, (B) Top-view, (C) Reflected G-shape

The simulated results of the three (3) iteration of the proposed Bio-EBG-iwA are as shown in Figure 4. It can be seen that the initiator (Figure 2(A)) has a wide band with a bandwidth of 2.13 GHz (4.72 – 6.85 GHz) at 10 dB return loss. Hence, cover the entire 5 GHz WLAN band (5.2 and 5.8 GHz). In the same light, the introduction of the reflected G-shape slit on the radiation patch leads to a band-notch at 2.6 GHz as predicted using Equation (4) and thereby leads to resonance at 2.42 GHz as shown in Figure 4. But, as it can be noticed, the impedance matching at 2.42 GHz is poor, which makes the return loss to be at 2.85 dB. Therefore, a stub at the ground plane is used to improve the impedance matching at the low-frequency band; which in turn reduces the bandwidth at the upper-frequency band as shown in Figure 4. The final configuration (III) has a resonance at 2.45 and 5.7 GHz with a reflection coefficient of −23.04 and −20.18 dB, respectively.

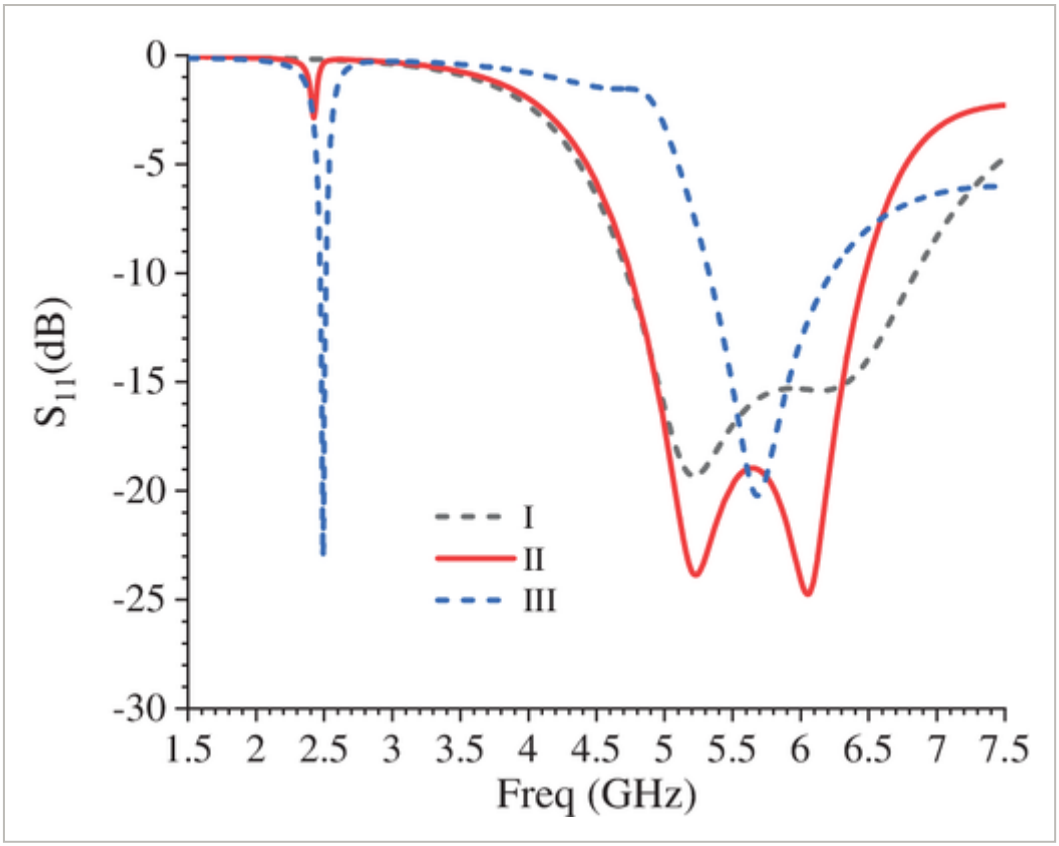

FIGURE 4

Open in figure viewer | PowerPoint

Simulated S_{11} of the bio-EBG-iwA design stages

In order to validate the final configuration, a prototype was fabricated and measured as shown in Figure 5. The radiating patch and the ground plane (Copper tape) shapes were cut using Roland® CAMM-1 GS-24 vinyl cutter and the substrate was cut using a RUNJI® cutter. It can be observed that the proposed bio-inspired antenna simulation and measurement results are in good agreement as shown in Figure 6

FIGURE 5

The prototype of the bio-EBG-iwA

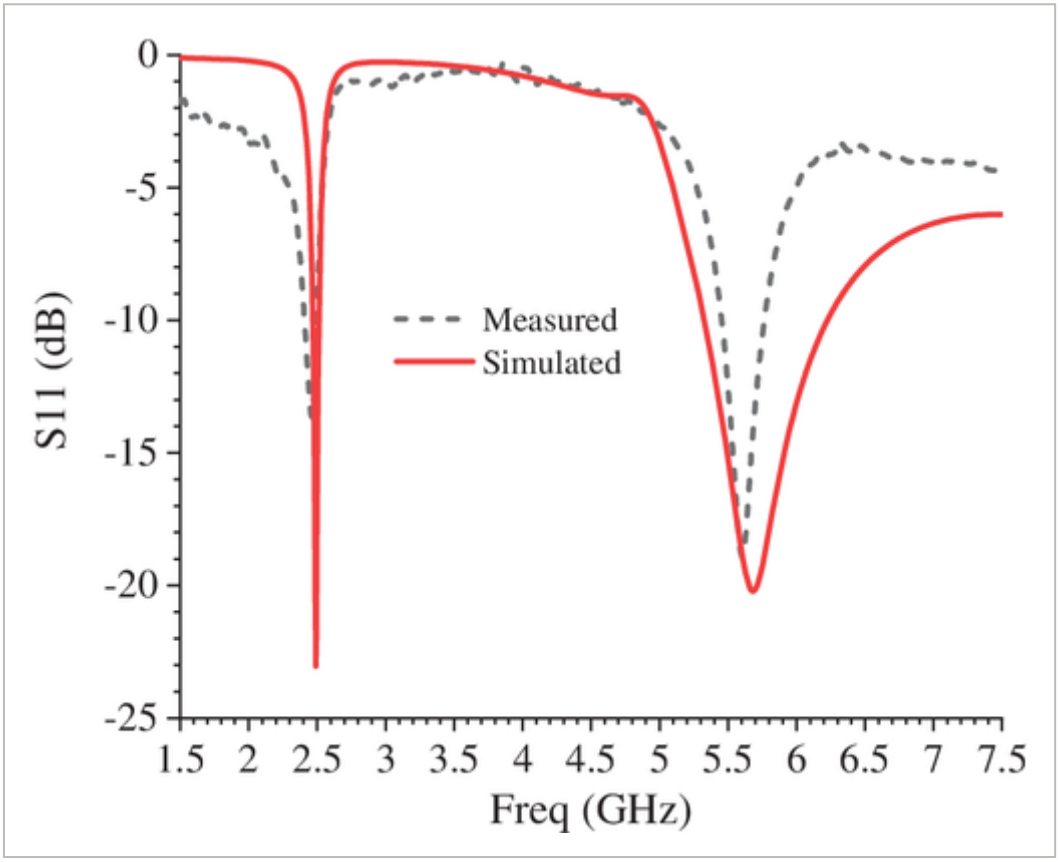

FIGURE 6

Measured and simulated S_{11} of the bio-EBG-iwA

2.2 Proposed uniplanar electromagnetic bandgap

The antenna designed for a wireless body area network (WBAN) should be less harmful to the user as well as less susceptible to the effect of human tissues. It is well known that monopole antenna normally suffers from back radiation, which in turn leads to severe degradation when brought close to the human body. Therefore, to avert these issues, artificial magnetic conductor (AMC) has been widely used to create isolation between the antenna and the body. In this work, a novel dual-band via-less EBG (uniplanar EBG) is proposed. The design is realized from a standard square patch on the *Aso-oke* textile of 2.1 mm thickness with a dielectric constant and a loss tangent of 1.43 and 0.019, respectively. The EBG design is based on a modified square-ring and a 90° rotated H-shape patch for the realization of the dual-band EBG,

respectively. The steps of realizing the proposed UC-EBG are shown in Figure 7(A-E). The dimension of the unit cell of the proposed uniplanar EBG and its equivalent circuit is as shown in Figures 8 and 9, respectively. The optimized dimension of the proposed EBG is presented in Table 2. It should be mentioned here that the proposed structure gives a high degree of design freedom to the engineers and comfort to the users because of its via-less configuration compared to mushroom EBG which usually causes user's discomfort. The inductance and the capacitance of the standard square patch AMC can be determined using Equations ((8) and (9))[8, 22]:

$$L = \mu H \tag{8}$$

$$C = \frac{W\varepsilon_o(1+\varepsilon_r)}{\pi}\cosh^{-1}\left(\frac{W+g}{g}\right) \tag{9}$$

where μ is the permeability of the material, H is the thickness of the substrate, W is the patch width, ε_o and ε_r are the free space and material permittivity respectively, g is the gap between two adjacent cells.

FIGURE 7

Open in figure viewer | PowerPoint

The unit cell design procedure of the proposed uniplanar flexible EBG

FIGURE 8

Open in figure viewer | PowerPoint

The unit cell of the proposed uniplanar flexible EBG

FIGURE 9

Open in figure viewer | PowerPoint

The equivalent circuit of the proposed EBG unit cell

It can be observed in Figure 9 that the initiator (square patch) has one zero reflection phase at 3.14 GHz and bandwidth of 0.38 GHz at ±90°.[17, 23] The ±90° is the phase where the free space impedance is less than the surface impedance of the structure.[23] In the Equivalent circuit of the proposed unit cell, L_1 , L_2 , L_3 , L_4 , C_1 , C_2 , and C_3 represent the inductance due to the reflected H-shape patch, the inductance due to the modified ring, the inductance due to the ground plane, the inductance due to the inset strip joining the adjacent patches, the capacitance between the Reflected H-shaped patch and the ground plane, the capacitance between the modified square ring and the ground plane and the capacitance between the reflected H-shaped and the modified square ring. The inductance of the modified square ring can be calculated from Equation (10). Other parameters can be calculated using Equations (8) and (9-8) and (9).

$$L_2 = (W - 12l_2)\frac{\mu_0}{4\pi} ln\left[1 + \frac{32h^2}{w_7^2}\left(1 + \sqrt{1 + \left(\frac{\pi w_7^2}{8h^2}\right)^2}\right)\right] \tag{10}$$

It can be observed in Figure 10(A) that the slit edges extended the electrical length of the patch and thereby reduces the zero-phase reflection coefficient from 3.14 to 2.86 GHz which is an 8.92% reduction. It can also be observed that the introduction of the center slot to realize reflected H-shaped (Figure 7(D)) leads to a tri-band zero-reflection phases at 2.37, 5.67, and 5.91 GHz. Nonetheless, the bandwidth at 5.67 and 5.91 GHz is extremely small as seen in Figure 10(A). On the contrary, when the middle strips are introduced on the slitted edge of the ring, the resulted configuration leads to a dual-band EBG at 2.45 and 5.68 GHz with a bandwidth of 0.13 GHz (2.38–2.51) GHz and 0.30 GHz (5.51–5.81) GHz at ±90°, respectively which are suitable for ISM and WLAN bands respectively as shown in Figure 10(A). It is important to state at this point that, the proposed structure can be easily modified to realize multiband EBG by varying the value of the design parameters (e.g., w_4 , w_6 , and l_2). In order to investigate our assumption that the outer ring is majorly responsible for the EBG operation at 2.45 GHz and the reflected H-shaped is responsible for the 5.68 GHz, the surface current distributions at these frequencies are presented in Figure 11(A,B), respectively. It can be observed that at 2.45 GHz, the surface current concentrates on the outer modified ring while the current concentrates on the reflected H-shaped at 5.68 GHz.

FIGURE 10

(A) The reflection phase of the EBG unit cell, (B) 3 × 3 suspended transmission line configuration, and (C) the transmission and reflection response

FIGURE 11

The surface current distribution on the EBG unit cell at (A) 2.45 GHz and (B) 5.68 GHz

In order to characterize the bandgap property of the UC-EBG proposed in this work, a suspended transmission line approach was used. The transmission line is suspended on a 3 × 3 array of the proposed flexible UC-EBG as shown in Figure 10(B) at a gap of 0.7 mm. The reflection and transmission responses are as shown in Figure 10(C). It can be observed that the S_{21} (dB) are less than –15 dB with a corresponding higher S_{11}(dB) at 2.45 and 5.7 GHz, respectively. It can be observed that the transmission coefficient is lower at the 5.7 GHz band than 2.45 GHz as shown in Figure 10(C). This implies that the surface wave will be suppressed better at the 5.7 GHz band than at 2.45 GHz. Therefore, it can be predicted that the antenna placed on the proposed UC-EBG structure will show better performance at 5.7 than 2.45 GHz.

3 ANTENNA PERFORMANCE OVER EBG

The ultra-compact wearable antenna designed in Section 1.1 is placed over a 2 × 2 array of the EBG presented in Section 1.2. The overall dimension of the proposed EBG integrated antenna is 69 × 69 × 6.04 mm^3. A foam of 3 mm is placed between the antenna and the EBG to isolate the antenna from being short-circuited. The top-view and the front-view of the proposed EBG integrated antenna are as shown in Figure 12(A,B), respectively. A 2 × 2 EBG array is fabricated as shown in Figure 13.

FIGURE 12

The configuration of the EBG integrated antenna (A) top view (B) front view

FIGURE 13

The 2 × 2 EBG configuration (A) top view (B) bottom view

3.1 Performance of the EBG integrated antenna in free space

3.1.1 Simulated and measured reflection coefficient (S_{11})

The antenna is placed on the EBG and simulated using an HFSS® which is based on the Finite Element method of solving maxwell equations. The simulated and the measured reflection coefficient of the integrated antenna in free space is as shown in Figure 14. A good agreement can be observed between the simulated and measured S_{11} (dB). It can be observed that the antenna without EBG resonates at 2.45 and 5.7 GHz with a return loss of 23.04 and 20.18 dB, respectively, while the EBG integrated antenna also resonates at 2.45 and 5.7 GHz but with an improved return loss of 24 and 29.45 dB at 2.45 and 5.7 GHz, respectively. This is the expected result as the surface wave is minimized, the return loss is expected to be enhanced as demonstrated in Figure 14. It is also worth noting that there is a small variation between the bandwidth of the simulated and measured at −10 dB. This can be traced to the losses contributed by the connectors and the fabrication error. Nonetheless, it can be observed that there is a good agreement between the simulated and measured results.

FIGURE 14

Open in figure viewer | PowerPoint

Simulated and measured reflection coefficient of the proposed bio-inspired antenna with (w/t) and without (w/o) EBG integrated

3.1.2 Gain, radiation pattern, and efficiency with and without EBG

The gain of the Bio-EBG-iwA with and without EBG at 2.45 and 5.7 GHz are as shown in Figure 15(A,B) respectively. As it can be seen in Figure 15(A), the peak gain of the antenna without the EBG at 2.45 GHz is −0.48 dBi while the EBG integrated Antenna has a peak gain of 5.9 dBi at the same frequency as shown in Figure 15(B); which implies a 6.38 dBi increase at 2.45 GHz. In the same light, at 5.7 GHz, the peak gain of the unloaded antenna is 2.5 dBi while that of the EBG integrated antenna has a peak gain of 10.7 dBi at the same frequency as shown in Figure 15(A,B), respectively which implies an 8.2 dBi increase. These results demonstrate the efficiency of the proposed EBG structure in comparison with the recently proposed structure in the literature. More so, for a clearer view of the radiation pattern, Figure 16(A,B) show the 2D radiation pattern of the proposed configuration with and without EBG at 2.45 and 5.7 GHz respectively.

FIGURE 15

Open in figure viewer | PowerPoint

3D simulated gain of the bio-EBG-iwA at 2.45 and 5.7 GHz (A) without EBG (B) with EBG

FIGURE 16

Open in figure viewer | PowerPoint

2D simulated radiation pattern of the bio-EBG-iwA with/without EBG at (A) 2.45 GHz and (B) 5.7 GHz

It can be observed from Figure 16(A,B) that the antenna without the EBG has a bi-directional radiation pattern at 2.45 GHz and a dumb-bell radiation pattern at 5.7 GHz on E-plane, respectively, while the H-plane radiation pattern at both frequencies is Omnidirectional. The use of the EBG converted the radiation pattern at both frequencies to a directional radiation pattern as shown in Figure 16(A,B). It can be observed from Figure 16 that the back radiation at 2.45 GHz is higher than the back radiation at 5.7 GHz. This can be related to the surface impedance of the EBG structure at these frequencies. The front-to-back ratio (FBR) radiation at 2.45 and 5.7 GHz is 7.37 and 26.29 dB, respectively. These justify the peak gain achieved at these frequencies. It is worth noting at this point that, as far as we know, 26.29 dB FBR presented in this work is the highest FBR achieved with single element compact antenna in the open literature. The radiation efficiency of 88.97% and 79.85% are achieved with the integration of EBG at 2.45 and 5.7 GHz, respectively. The far-field performance analysis presented in this section shows that the proposed EBG integrated antenna designed and fabricated on a locally made textile material is a suitable candidate for medical and military application in a body area network.

In order to show that the EBG is responsible for the performance enhancement, the same configuration with the replacement of the EBG with perfect electric conductor (PEC) surface was simulated as shown in Figure 17. It can be seen in Figure 18 that it adversely affects the antenna performance. The simulated gain at 2.45 and 5.7 GHz is 3.68 and 9.78 dBi which are less than the gain achieved with the EBG. The efficiency of the PEC-based antenna also degraded to 20% and 78% at 2.45 and 5.7 GHz respectively. Therefore, it can be seen that our proposed EBG design works as a High impedance surface instead of a PEC surface.

FIGURE 17

Open in figure viewer | PowerPoint

Antenna on PEC surface

FIGURE 18

Open in figure viewer | PowerPoint

S_{11} of the Antenna on PEC surface

3.2 Bio-EBG-iwA on-body analysis with and without EBG

The on-body analysis of a wearable antenna is an important aspect analysis because of the noisy nature of human tissues which can degrade the antenna performance when brought close to the body. In order to evaluate the on-body performance of Bio-EBG-iwA, a flat 4-layered model of the human body tissue is used which consists of skin, fat, muscle, and bone as shown in Figure 19(A). Figure 19(B,C) show the antenna alone and the EBG integrated antenna is placed on the human-tissue model (HTM) at the distance of 2 mm, respectively. The human-body model parameters are given in Table 3.

FIGURE 19

Open in figure viewer | PowerPoint

The on-body analysis configuration (A) the HTM (B) antenna on the HTM (C) EBG integrated antenna on the HTM

TABLE 3. Properties of the human-tissue model[8, 10]

	Bone	Skin	Fat	Muscle
Thickness (mm)	13	2	5	20
ε_r	18.49	37.95	5.27	52.67
σ (S/m)	0.82	1.49	0.11	1.77
Density (kg/m^3)	1008	1001	900	1006

3.2.1 On-body reflection coefficient with and without EBG

The off-body and on-body S_{11} of the Bio-EBG-iwA with and without EBG is as shown in Figure 20. It can be observed that there is high-frequency detuning from 2.45 and 5.7 GHz to 1.95 and 5.15 GHz when the antenna is placed on the HTM, respectively. It can also be observed that there is a broadening of the bandwidth at the upper band from 0.9 GHz (5.3–6.2 GHz) to 2.3 GHz (3.8 – 6.1 GHz). This implies that the proposed antenna cannot actually be used in the ISM band when placed directly on the body. On the other hand, when the antenna is placed on the EBG before placing on the HTM, no significant detuning is observed at 2.45 and 5.7 GHz, respectively. Even though there is a small shift from 5.7 to 5.8 GHz at the upper band, yet it is within the desired frequency. It is worth noting also that the bandwidth at 5.7 GHz is reduced in the on-body application. Nonetheless, the bandwidth is within the acceptable range. Therefore, the proposed EBG integrated antenna meets the requirements for an on-body WBAN application.

FIGURE 20

Open in figure viewer | PowerPoint

On-body and free-space S_{11} of the bio-EBG-iwA with (w/t) and without (w/o) EBG

The on-body S_{11} measurement of EBG integrated antenna on the human body is carried out on a volunteer. He has a height of 5.7 m, a weight of 60 kg, and a light complexion. The EBG integrated antenna is placed on the chest, arm, and forehead as shown in Figure 21(A-C), respectively. The measured S_{11} of the on-body configuration is as shown in Figure 22. It can be observed that the resonances at 2.45 and 5.7 GHz are maintained throughout. This shows that Bio-EBG-iwA is fit for all body area communication without location discrimination.

FIGURE 21

Open in figure viewer | PowerPoint

The setup for S_{11} measurement of the bio-EBG-iwA on human body (A) Chest, (B) Arm, and (C) Forehead

FIGURE 22

Open in figure viewer | PowerPoint

The on-body measured S_{11} on the chest, arm, and forehead

3.2.2 Radiation pattern, gain, and efficiency with and without EBG

Figure 23(A,B) show the on-body as well as the free space radiation patterns of the Bio-EBG-iwA with and without EBG. It can be observed that there is no significant effect on the radiation pattern of the EBG integrated antenna in both E-plane and H-plane at 2.45 GHz as well as at 5.7 GHz when placed on HTM. On the contrary, a significant change is observed in the radiation pattern of the antenna without the EBG degraded with HTM proximity. The efficiency of the antenna in the on-body application with EBG at 2.45 GHz degraded from 88.97% to 45.0%. Also, at 5.7 GHz, the efficiency of the antenna with EBG degraded from 79.85% to 58%. This clearly shows that HTM has a degrading effect on the EBG-backed antenna. Nonetheless, it is within the acceptable performance.

FIGURE 23

Open in figure viewer | PowerPoint

On-body and free-space radiation pattern of bio-EBG-iwA with (w/t) and without (w/o) EBG at (A) 2.45 GHz and (B) 5.7 GHz

3.2.3 Specific absorption ratio analysis

In wearable devices, the safety of the users is of the highest priority; most especially in wearable antenna due to the effect of the EM radiation on human health. Specific absorption ratio (SAR) is the parameter of safety, which shows the amount of electromagnetic field absorbed by the human body. This performance analysis must be carried out to ensure that the users are safe. According to the regulatory standard given by the FCC and ICNIRP, 1.6 W/kg for an average of 1 g of tissue and 2 W/kg for the average greater than 10 g of tissue. In order to evaluate the SAR of the Bio-EBG-iwA, a space of 2 mm is ensured between the HTM and the antenna. A 100 mW power is used as input power and the IEEE/IEC Std 62 704 standard, given in HFSS, is used in this work. The SAR is evaluated at both 2.45 and 5.7 GHz using 1 g of tissue. Figure 24(A,B) show the SAR at 2.45 and 5.7 GHz without and with EBG respectively. The antenna without the EBG-backed has an average SAR of 15.4 and 25.17 W/kg at 2.45 and 5.7 GHz respectively. But, for UC-EBG integrated antenna, the average SAR is 0.26 and 0.15 W/kg at 2.45 and 5.7 GHz, respectively. Therefore, with the use of the proposed UC-EBG, there is a 98.31% and 99.4% reduction in average SAR at 2.45 and 5.7 GHz, respectively. Since the average SAR at 2.45 and 5.7 GHz is much below the minimum acceptable value, the Bio-EBG-iwA is applicable in WBAN communication.

FIGURE 24

Open in figure viewer | PowerPoint

The SAR of the bio-EBG-iwA with/without EBG at (A) 2.45 and (B) 5.7 GHz for 1 g of tissue at a 2 mm distance from the skin

4 COMPARATIVE ANALYSIS OF BIO-EBG-IWA WITH SOME PUBLISHED WORKS

The Bio-EBG-iwA proposed in this work is compared with some of the recently published works and presented in Table 4. In order to ensure a fair comparison, the guided wavelength at the lowest resonant frequency is used to express the antenna and EBG dimensions. It should be noted that authors in Refs. 6, 24 did not use either full ground or High impedance surface which eventually made the antenna proposed in their work less suitable for On-body application as the antenna performance degraded when in close-proximity with HTM. It is also worth noting that even though the overall size of the antenna proposed by the authors in Ref. 8 is small compared to our Bio-EBG-iwA, yet the efficiency of their proposed antenna was not reported which raises a question as to the workability of the antenna when in closed proximity to HTM. The same issue applies to the work reported in Ref. 25. It can also be observed from Table 4 that the antenna proposed in Refs. 8, 10 are single band antennas compared to our proposed Bio-EBG-iwA which is dual-band. It can be seen that the Bio-EBG-iwA outperformed the recently published antenna in terms of antenna compactness, FBR, gain, and radiation efficiency. It is therefore a suitable candidate for wearable applications.

TABLE 4. Comparative analysis of bio-EBG-iwA with some published works

References	Year	Ant. size (λ_g^3)	EBG period (λ_g)	Overall size (λ_g^3)	Freq. (GHz)	FBR (dB)	Gain (dBi)	Eff. (%)	Flexibility
6	2020	0.2 × 0.3 × 0.009	—	Same as Ant.	2.4	NR	2.5	93	Semi-flex
24	2020	0.44 × 0.49 × 0.015	—	same as Ant.	1.2/1.5/2.4/3.4	NR	1.75/3/6/3	86	Flex

References	Year	Ant. size (λ_g^3)	EBG period (λ_g)	Overall size (λ_g^3)	Freq. (GHz)	FBR (dB)	Gain (dBi)	Eff. (%)	Flexibility
		× 0.75 × 0.01		1.38 × 0.15					

5 CONCLUSION

A novel ultra-compact bio-inspired UC-EBG backed antenna (Bio-EBG-iwA) is presented in this work. It has been demonstrated that the proposed Bio-EBG-iwA antenna, which operates at 2.45 and 5.7 GHz, outperformed the recently proposed wearable antennas in the literature in terms of antenna size, gain, radiation efficiency, and FBR. Therefore, it is a suitable candidate for wearable and future WBAN applications such as medical and military.

ACKNOWLEDGMENTS

This work was sponsored and supported by the African Union through the Pan African University Institute of Basic Sciences, Technology, and Innovation.

Biographies

Jeremiah O. Abolade received his B.Sc. and M.Sc. degrees in Electrical and Electronic Engineering from the University of Ibadan in 2012 and 2016, respectively. He was a Lecturer and a member of the 5G research group at Covenant University, Ota, Nigeria from 2017 to 2018. He is also a member of the microwave systems research group, Nairobi, Kenya. He is a graduate student member of IEEE, and a member of the Nigerian Society of Engineers (NSE). He is presently a Ph.D. scholar at the Pan African University Institute for Basic Sciences, Technology and Innovation, hosted at Jomo Kenyatta University of Technology and Agriculture, Nairobi, Kenya. He has published in both local and highly referred international journals. His current research interests include compact multiband antennas and metamaterial for future wireless applications.

Dominic B. O. Konditi was born on July 22, 1950, in Kochia, Homa-Bay District, Kenya. He received his Ph.D. in Electronics and Computer Engineering from Indian Institute of Technology (IIT), Roorkee, in 2000, Masters of Engineering degree in Electrical Engineering from Tottori

University, Japan in 1991. He has authored several papers in refereed journals and conference proceedings. In 2003, he received the best paper award for his paper published in the Institution of Electronics & Telecommunications Engineers (IETE) journal in New Delhi, India. He has been a reviewer of Radio Science Geophysical Society Journal (Washington DC), The New Measurements and Instrumentation Journal, WSEAS Journals and Conference Proceedings (Athens, Greece), ENMA Conference proceedings (Bilbao, Spain), SAIEEE Africa Research Journal (South Africa), and JAGST journal (Nairobi, Kenya). He is currently the Chair of, Kenya Society of Electrical & Electronic Engineers (KSEEE). He has been an external examiner for Moi University and Masinde University of Science & Technology (MMUST), both in Kenya, and the University of Kwa-Zulu Natal, Durban, South Africa. Prof. Konditi has been cited in Marquis WHO'S WHO in Science and Engineering and Cambridge Bibliographic Society, England. His research interests are in Computational Electromagnetics, numerical techniques for waveguides, conducting screens and micro-strip lines and apertures as pertains to EMC/EMI and biomedical engineering. He is a member of IEEE, WSEAS (Greece), KSEEE (Kenya), and the Associate Member of IEK (Kenya).

Vasant. M. Dharmadhikary (Member, IEEE) was born on July 24, 1948. He received the Bachelor of Engineering (B.E.) in 1971 and the Masters of Engineering (M.E.) in 1974, both from the University of Poona, India. He is a lecturer of longstanding with over 30 years of experience. He has published several papers in journals and conference proceedings. His interests are in the areas of electromagnetics and religious studies. He is a life member of the Indian Science Congress Association and member of the Indian Society for Technical Education, Institution of Electrical & Electronic Engineers, Kenya National Association of Physicists, and the Academic Board of Kenya Institute of Education. He is currently a member of IEEE, the Indian Society for Technical Education, and a member of Kenya National Association of Physicists Kenya. His associate professor of Electrical Engineering at Department of Electrical and Electronic Engineering, Dedan Kimathi University of Technology, Nyeri, Kenya. His research interests include antenna design for future communication, Computational Electromagnetic, EMC/EMI problems.

Open Research

DATA AVAILABILITY STATEMENT

Data sharing is not applicable to this article as no new data were created or analyzed in this study.

REFERENCES

1 P. K. D. Pramanik, A. Nayyar, and G. Pareek, WBAN: Driving e-healthcare beyond telemedicine to remote health monitoring: architecture and protocols. Elsevier Inc., 2019.
Google Scholar

2 Ferreira D, Pires P, Rodrigues R, Caldeirinha RFS. Wearable textile antennas: examining the effect of bending on their performance. *IEEE Antennas Propag Mag*. 2017; **59**(3): 54- 59.
https://doi.org/10.1109/MAP.2017.2686093
Crossref | Web of Science® | Google Scholar

3 Sreelakshmi K, Rao GS, Kumar MNVSS. A compact grounded asymmetric coplanar strip-fed flexible multiband reconfigurable antenna for wireless applications. *IEEE Access*. 2020; **8**: 497- 507.
https://doi.org/10.1109/ACCESS.2020.3033502
Crossref | Web of Science® | Google Scholar

4 Yadav A, Singh VK, Bhoi AK, Marques G, Garcia-Zapirain B. Wireless body area networks: UWB wearable textile antenna for telemedicine and mobile health systems. *Micromachines*. 2020; **11**(6): 1-22. https://doi.org/10.3390/MI11060558
Crossref | CAS | Web of Science® | Google Scholar

5 A. Sabban, Small wearable antennas for wireless communication and medical systems. Paper presented at: 2018 IEEE Radio and Wireless Symposium (RWS), 2018, pp. 161– 164, doi: https://doi.org/10.1109/RWS.2018.8304974 .
Google Scholar

6 Smida A, Iqbal A, Alazemi AJ, Waly MI, Ghayoula R, Kim S. Wideband wearable antenna for biomedical telemetry applications. *IEEE Access*. 2020; **8**: 687- 694.
https://doi.org/10.1109/aCCESS.2020.2967413
Crossref | Web of Science® | Google Scholar

7 Paracha KN, Abdul Rahim SK, Soh PJ, Khalily M. Wearable antennas: a review of materials, structures, and innovative features for autonomous communication and sensing. *IEEE Access*. 2019; **7**: 694- 712. https://doi.org/10.1109/ACCESS.2019.2909146
Crossref | Web of Science® | Google Scholar

8 Ashyap AYI et al. Compact and low-profile textile EBG-based antenna for wearable medical applications. *IEEE Antennas Wirel Propag Lett*. 2017; **16**: 2550- 2553.
https://doi.org/10.1109/LAWP.2017.2732355
Crossref | Web of Science® | Google Scholar

9 Mandal D, Pattnaik SS. Wide CPW-fed multiband wearable monopole antenna with extended grounds for GSM/WLAN/WiMAX applications. *Int J Antennas Propag*. 2019; **2019**: 4264513.

https://doi.org/10.1155/2019/4264513
Crossref | Web of Science® | Google Scholar

10 Ashyap AYI et al. Robust and efficient integrated antenna with EBG-DGS enabled wide bandwidth for wearable medical device applications. *IEEE Access*. 2020; **8**: 346- 358. https://doi.org/10.1109/ACCESS.2020.2981867
Crossref | Web of Science® | Google Scholar

11 Sievenpiper D, Zhang L, Jimenez Broas RF, Alexöpolous NG, Yablonovitch E. High-impedance electromagnetic surfaces with a forbidden frequency band. *IEEE Trans Microw Theory Tech*. 1999; **47**(11): 2059- 2074. https://doi.org/10.1109/22.798001
Crossref | Web of Science® | Google Scholar

12 Li A, Singh S, Sievenpiper D. Metasurfaces and their applications. *Nanophotonics*. 2018; **7**(6): 989-1011. https://doi.org/10.1515/nanoph-2017-0120
Crossref | Web of Science® | Google Scholar

13 I. M. M. Yusoff, N. M. Salleh, A. A. Azlan, R. A. Awang, and M. T. Ali, Radiated electromagnetic bad gap antenna for ISM band in medical application. Paper presented at: 2018 IEEE International RF and Microwave Conference (RFM), 2018, pp. 103– 106, doi: https://doi.org/10.1109/RFM.2018.8846532 .
Google Scholar

14 Inum R, Rana MM, Shushama KN, Quader MA. EBG based microstrip patch antenna for brain tumor detection via scattering parameters in microwave imaging system. *Int J Biomed Imag*. 2018; **2018**: 1- 12. https://doi.org/10.1155/2018/8241438
Crossref | Web of Science® | Google Scholar

15 Mersani A, Lotfi O, Ribero JM. Design of a textile antenna with artificial magnetic conductor for wearable applications. *Microw Opt Technol Lett*. 2018; **60**(6): 1343- 1349. https://doi.org/10.1002/mop.31158
Wiley Online Library | Web of Science® | Google Scholar

16 Shen Y. Minimized low-profile wideband antennas using high impedance surface. *Int J Antennas Propag*. 2017; **2017**: 2563927. https://doi.org/10.1155/2017/2563927
Crossref | Web of Science® | Google Scholar

17 A. Z. Babar and A. Z. Babar, Design and simulation of dual band EBG. Paper presented at: 2017 14th International Bhurban Conference on Applied Sciences and Technology (IBCAST), 2017, pp. 727–731, doi: https://doi.org/10.1109/IBCAST.2017.7868133 .
Google Scholar

18 Dewan R, Rahim MK, Hamid MR, Himdi M, Majid HA, Samsuri NA. HIS-EBG unit cells for pattern and frequency reconfigurable dual band array antenna. *Prog Electromagn Res*. 2018; **76**: 123- 132.

Crossref | Web of Science® | Google Scholar

19 Lin MS, Huang YH, Hsu CIG. Design a dual-band high-impedance surface structure for electromagnetic protection in WLAN applications. *IEEE Int Symp Electromagn Compat*. 2014; **2014**: 525-528.
Google Scholar

20 Abolade JO, Konditi DBO, Dharmadhikary VM. Comparative study of textile material characterization techniques for wearable antennas. *Results Mater*. 2021; **9**:168.
https://doi.org/10.1016/j.rinma.2021.100168
Google Scholar

21 Abolade JO, Konditi DBO, Dharmadhikary VM. Compact hexa-band bio-inspired antenna using asymmetric microstrip feeding technique for wireless applications. *Heliyon*. 2021; **7**(2):e06247.
https://doi.org/10.1016/j.heliyon.2021.e06247
Crossref | PubMed | Google Scholar

22 Zhang X, Teng Z, Liu Z, Li B. A dual band patch antenna with a pinwheel-shaped slots EBG substrate. *Int J Antennas Propag*. 2015; **2015**: 815751. https://doi.org/10.1155/2015/815751
Crossref | Web of Science® | Google Scholar

23 Ashyap AYI et al. An overview of electromagnetic band-gap integrated wearable antennas. *IEEE Access*. 2020; **8**: 7641- 7658. https://doi.org/10.1109/ACCESS.2020.2963997
Crossref | Web of Science® | Google Scholar

24 B. B. Q. Elias, P. J. Soh, A. A. Al-Hadi, R. Joshi, Y. Li, and S. K. Podilchak, Design of a quad band CPW-fed compact flexible patch antenna for wearable applications. Paper presented at: 2020 14th European Conference on Antennas and Propagation (EuCAP), 2020, pp. 1– 5.
https://doi.org/10.23919/EuCAP48036.2020.9135261
Google Scholar

25 Mu G, Ren P. A compact dual-band metasurface-based antenna for wearable medical body-area network devices. *J Electr Comput Eng*. 2020; **2020**: 4967198. https://doi.org/10.1155/2020/4967198
Web of Science® | Google Scholar

26 Gao G, Wang S, Zhang R, Yang C, Hu B. Flexible EBG-backed PIFA based on conductive textile and PDMS for wearable applications. *Microw Opt Technol Lett*. 2020; **62**(4): 1733- 1741.
https://doi.org/10.1002/mop.32224
Wiley Online Library | Web of Science® | Google Scholar

Download PDF